Majority Rule in Nonlinear Opinion Dynamics

Michael Gabbay and Arindam K. Das

Abstract Using a nonlinear model of opinion dynamics on networks, we show the existence of asymmetric majority rule solutions for symmetric initial opinion distributions and symmetric network structure. We show that this occurs in triads as the result of a pitchfork bifurcation and arises in both chain and complete topologies with symmetric as well as asymmetric coupling. Analytical approximations for bifurcation boundaries are derived which closely match numerically-obtained boundaries. Bifurcation-induced symmetry breaking represents a novel mechanism for generating majority rule outcomes without built-in structural or dynamical asymmetries; however, the policy outcome is fundamentally unpredictable.

1 Introduction

Small group opinion change has long been a subject of intense study in social science with implications for decision making by a range of groups such as political leaders, judicial panels, corporate committees, and juries [4, 8]. Mathematical models of small group decision making have been proposed in social science disciplines such as psychology, sociology, political science, economics, and law [2, 5, 9]. In this paper, we put forth a novel mechanism for the generation of majority rule outcomes in small groups via a symmetry-breaking pitchfork bifurcation. This mechanism allows for asymmetric outcomes to appear for symmetric initial opinion distributions even when group members are symmetrically coupled. It occurs in the nonlinear opinion dynamics model of Refs. [6, 7] under conditions of high disagreement between the

M. Gabbay(✉)
Applied Physics Laboratory, University of Washington, Seattle, WA 98105, USA
e-mail: gabbay@uw.edu

A. K. Das
Department of Engineering and Design, Eastern Washington University, Cheney, WA 99004, USA
e-mail: arindam@uw.edu

V. In et al. (eds.), *International Conference on Theory and Application in Nonlinear Dynamics (ICAND 2012)*, Understanding Complex Systems,
DOI: 10.1007/978-3-319-02925-2_15,

ends of the distribution along a continuous opinion axis. For example, in a triad network consisting of a centrist bracketed by two opposed extremists, the centrist will form a majority pair with one of the extremists. This runs counter to intuition rooted in basic psychological mechanisms of attitude change which emphasize a convergence process of group member attitudes, and so would anticipate either deadlock or various degrees of compromise around the centrist's position, but not majority rule. In particular, it is not predicted by the most prominent network-based model of small group opinion dynamics, the Friedkin-Johnsen model, which is linear in the disagreement between group members [5]. The Friedkin-Johnsen and nonlinear opinion dynamics models are described in the next section. The majority rule outcome for a triad is demonstrated in simulation (Sect. 3) and via bifurcation analysis (Sect. 4). Majority rule in five-node networks is presented in Sect. 5.

2 Opinion Dynamics Models

Most recent work on opinion network dynamics in the physics community has focused on large networks motivated by an interest in population scale dynamics [1]. Consensus in small networks has been studied in the literature on distributed network control with sensor networks as a primary motivation [10, 11]. However, our nonlinear model is most closely related to that of Friedkin and Johnsen, which was explicitly developed for the social influence context and has been subjected to empirical investigation [5].

2.1 Friedkin-Johnsen Model

The Friedkin-Johnsen model describes the temporal evolution of a linear discrete time influence process in a group of N people (nodes) as a weighted average of their previous opinions and their initial opinions [5]:

$$x_i(k+1) = a_i \sum_{j=1}^{N} w_{ij} x_j(k) + (1 - a_i) x_i(0); \quad i = 1, 2, \ldots N, k \geq 0, \qquad (1)$$

where $x_i(k)$ is the opinion of node i at time k; $x_i(0)$ is the initial opinion; a_i is the susceptibility of node i; and w_{ij} is the coupling weight scaling node j's influence upon i. The w_{ij} are non-negative and satisfy $\sum_{j=1}^{N} w_{ij} = 1$. In addition, the susceptibility is given by $a_i = 1 - w_{ii}$.

Equation (1) can be cast as a difference equation by subtracting $x_i(k) = (1 + a_i - a_i)x_i(k)$ from both sides and rearranging to yield

$$x_i(k+1) - x_i(k) = a_i \sum_{j=1}^{N} w_{ij}(x_j(k) - x_i(k)) - (1 - a_i)(x_i(k) - x_i(0)). \quad (2)$$

If $a_i = 1 \forall i$ in Eq. (2), then the node opinions will all converge to exactly the same value for a (bidirectionally) connected network. The presence of $x_i(0)$ in the dynamics of the Friedkin-Johnsen model prevents such a collapse onto an exact consensus which would signify the unintuitive complete extinction of disagreement. However, because of the linear coupling in the Friedkin-Johnsen model, equilibria in which the member opinions are asymmetrically distributed around the mean must arise from pre-existing asymmetries; either skewed initial opinion distributions or lopsided coupling weights in favor of one extreme. This is not the case for the nonlinear model which we turn to next.

2.2 Nonlinear Model

We use the following model for the evolution of the opinion x_i [7]:

$$\frac{dx_i}{dt} = -\gamma_i(x_i - \mu_i) + \sum_{j=1}^{N} \kappa_{ij} h(x_j - x_i). \quad (3)$$

The first term on the right is a linear "self-bias force" which expresses the psychological tension that a person feels if her opinion is displaced from her natural bias μ_i and is proportional to her commitment γ_i. The second term is the "group influence force" on i where κ_{ij} is the coupling strength and $h(x_j - x_i)$ is the coupling function. The coupling strength, which we take to be non-negative, represents the components of influence of j upon i arising from their relationship; it depends on factors such as how often j communicates with i and the regard with which i holds j. The coupling function represents how the influence of j upon i depends on the difference between their opinions. We use a dependence motivated by social judgment theory [4] in which the force grows for $|x_j - x_i| < \lambda_i$, where λ_i is is latitude of acceptance, but wanes for differences in excess of λ_i:

$$h(x_j - x_i) = (x_j - x_i) exp\left[-\frac{1}{2}\frac{(x_j - x_i)^2}{\lambda_i^2}\right]. \quad (4)$$

For situations in which a group first starts discussing an issue it is appropriate to use natural bias initial conditions, $x_i(0) = \mu_i$.

In the linear limit, $\lambda_i \to \infty$, it can readily be seen that the (discretized) nonlinear model reduces to the form (2) of the Friedkin-Johnsen model, apart from parameter constraints. The natural bias μ_i plays the same role in preventing the collapse onto exact agreement in (3) as the initial opinion does in (1). When applied to group

decision-making, we assume that a common decision can be reached between group members if their final opinions $x_i(t_f)$ are sufficiently close. This is in accord with the intuition that people need not precisely agree in order to reach a compromise decision on a common course of action.

3 Triad Simulations

We simulate a triad network in which the natural biases are symmetrically distributed around zero: $\mu_1 = -\Delta\mu/2$, $\mu_2 = 0$, and $\mu_3 = \Delta\mu/2$. We use a chain topology whose ends, nodes 1 and 3, are not connected so that the symmetric, binary adjacency matrix elements are $A_{12} = A_{21} = A_{23} = A_{32} = 1$ and $A_{13} = A_{31} = 0$ (and also $A_{ii} = 0$). However, the complete network in which all members are connected, $A_{ij} = 1 - \delta_{ij}$ where δ_{ij} is Kroneckers delta, has similar behavior as will be seen in Sect. 4. We use the parameter v to allow for the possibility of asymmetric coupling between the center node 2 and the end nodes so that $\kappa_{12} = \kappa_{32} = \kappa + v$ and $\kappa_{21} = \kappa_{23} = \kappa - v$ where $|v| < \kappa$. A positive value of v signifies that the center node has greater influence on each of the end nodes than vice versa whereas negative v signifies that the ends have more influence. The equations of motion for the triad are then:

$$\begin{aligned}
\frac{dx_1}{dt} &= -\left(x_1 + \frac{\Delta\mu}{2}\right) + (\kappa + v)h(x_2 - x_1) + \kappa A_{31} h(x_3 - x_1), \\
\frac{dx_2}{dt} &= -x_2 + (\kappa - v)(h(x_1 - x_2) + h(x_3 - x_2)), \\
\frac{dx_3}{dt} &= -\left(x_3 - \frac{\Delta\mu}{2}\right) + (\kappa + v)h(x_2 - x_3) + \kappa A_{31} h(x_1 - x_3).
\end{aligned} \tag{5}$$

It will be useful to define the following pair of variables: the *discord* $r = x_3 - x_1$, the opinion difference between the outer nodes and the *asymmetry* $s = (x_3 - x_2) - (x_2 - x_1)$, the difference in distances from the outer nodes to the middle node.

Figure 1 shows simulations of the chain network for three values of the coupling strength κ and with symmetric coupling between all nodes. The difference in the natural biases of the end nodes is $\Delta\mu = 5$ and the initial opinions are set equal to the natural biases (except for a tiny displacement to the center node as an initial perturbation which always moves x_2 in the same direction for the asymmetric solutions). Three qualitatively distinct equilibria are observed. At low coupling, Fig. 1a shows a state of Symmetric High Discord (SHD) in which the end nodes barely move from their natural biases and the center node remains at zero. At intermediate coupling, Fig. 1b shows the Majority Rule (MR) state in which the center node moves toward one of the end nodes to form a majority rule pair. At high coupling, the outer nodes move considerably toward the center to form a Symmetric Low Discord (SLD) state as shown in Fig. 1c. The SHD state corresponds to a deadlock situation in which

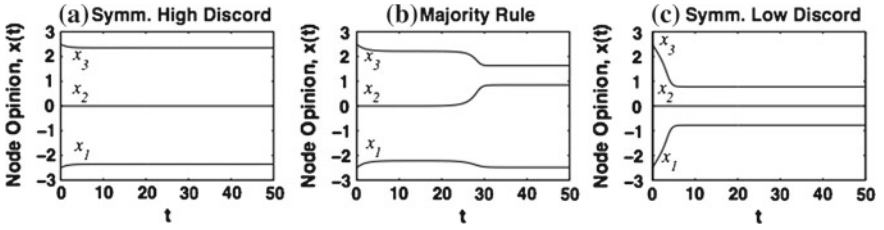

Fig. 1 Equilibrium outcomes in symmetrically-coupled ($v = 0$) triad chain network with high initial disagreement, $\Delta\mu = 5$, at different coupling strengths: **a** $\kappa = 1$, symmetric high discord; **b** $\kappa = 1.5$, majority rule; **c** $\kappa = 3$, symmetric low discord. Initial conditions: $x_1(0) = -2.5$, $x_2(0) = 10^{-6}$, $x_3(0) = 2.5$

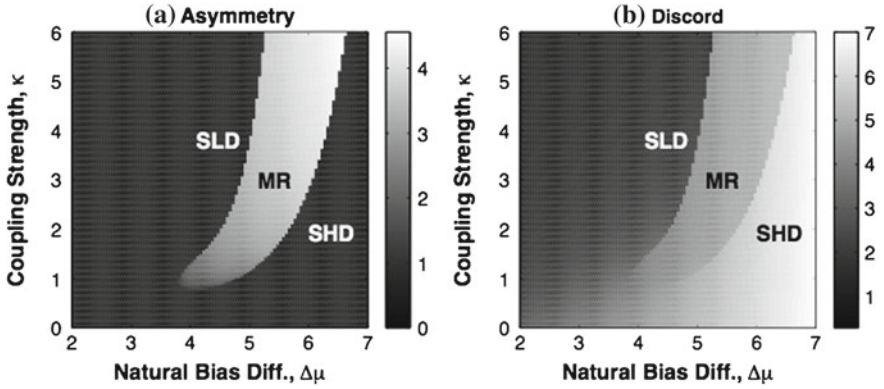

Fig. 2 Simulation of a symmetrically-coupled triad chain network over $\Delta\mu - \kappa$ parameter space showing final: **a** discord and **b** asymmetry (absolute value). Simulation duration is $t_f = 200$

all group members are far apart and no acceptable mutual decision can be made. In the MR state, the majority pair can likely agree on a common policy which will be the policy of the group if majority rule is sufficient for reaching a decision. In the SLD state, the distance between the outer nodes is much reduced and the basis for a compromise around the centrists position could be set. Simulations in which μ_1, μ_2, and μ_3 are randomly shifted by a small amount still display all three outcome types.

Figure 2 plots the asymmetry and discord of the symmetrically-coupled chain network with natural bias initial conditions. The emergence of the MR state only occurs past a critical value of the natural bias difference $\Delta\mu_c = 3.8$ which we call the *critical divergence*. Also, note the sharp discontinuities at the boundaries between the various outcome states. Below the critical divergence, asymmetric solutions do not exist and the discord is smoothly and symmetrically reduced as the coupling strength is raised as would occur in the equivalent case for the Friedkin-Johnsen model, for which the transition from deadlock to compromise to consensus is gradual with no possibility of an MR state.

4 Bifurcation Analysis for Triad

In this section, we show that the majority rule state is the result of spontaneous symmetry-breaking induced by a pitchfork bifurcation and we calculate bifurcation boundaries. We do this for the chain topology in which $A_{31} = 0$. We transform the system (5) into the discord and asymmetry variables, r and s, as well as the mean node opinion, $\bar{x} = \frac{1}{3}\sum_{i=1}^{3} x_i$. Using the fact that the coupling function is odd, $h(-x) = -h(x)$, results in the system:

$$\frac{dr}{dt} = -(r - \Delta\mu) - (\kappa + v)\left(h\left(\frac{r+s}{2}\right) + h\left(\frac{r-s}{2}\right)\right) \tag{6}$$

$$\frac{ds}{dt} = -s - (3\kappa - v)\left(h\left(\frac{r+s}{2}\right) - h\left(\frac{r-s}{2}\right)\right) \tag{7}$$

$$\frac{d\bar{x}}{dt} = -\bar{x} - \frac{2}{3}v\left(h\left(\frac{r+s}{2}\right) - h\left(\frac{r-s}{2}\right)\right) \tag{8}$$

For symmetric coupling, Eq. (8) implies that the mean equilibrium opinion is zero, the mean of the natural biases; this will not be the case for $v \neq 0$ in the MR state in which $s \neq 0$.

For the equilibrium SHD state, denoted by (r, s), the asymmetry is by definition $s = 0$. For large $\Delta\mu$ we take the discord to be $r \approx \Delta\mu + \theta$ where $\theta \ll 1$. Before showing the existence of the pitchfork bifurcation, it will be useful below to calculate θ . When $s = 0$, Eq. (6) becomes

$$\frac{dr}{dt} = -(r - \Delta\mu) - 2(\kappa + v)h\left(\frac{r}{2}\right), \tag{9}$$

which upon substituting the above form for r yields

$$0 = \theta + 2(\kappa + v)h\left(\frac{\Delta\mu + \theta}{2}\right). \tag{10}$$

Expanding the coupling function as $h(\frac{\Delta\mu+\theta}{2}) \approx h(\frac{\Delta\mu}{2}) + h'(\frac{\Delta\mu}{2})\frac{\theta}{2}$ and substituting into (10) enables us to solve for θ

$$\theta = -\frac{2(\kappa + v)h\left(\frac{\Delta\mu}{2}\right)}{1 + (\kappa + v)h'\left(\frac{\Delta\mu}{2}\right)} \tag{11}$$

where $h\left(\frac{\Delta\mu}{2}\right) = \frac{\Delta\mu}{2}e^{-\frac{\Delta\mu^2}{8}}$ and $h'\left(\frac{\Delta\mu}{2}\right) = \left(1 - \frac{\Delta\mu^2}{4}\right)e^{-\frac{\Delta\mu^2}{8}}$.

To show the bifurcation, we consider small perturbations s around $s = 0$ in Eq. (7). This results in the Taylor expansion,

$$\frac{ds}{dt} \approx -\left(1 + (3\kappa - v)h'\left(\frac{r}{2}\right)\right)s - \frac{1}{24}(3\kappa - v)h'''\left(\frac{r}{2}\right)s^3, \tag{12}$$

where only the odd power terms survive. When the coefficient of the linear term is positive, the symmetric state will be unstable. When $h'''(r/2) > 0$, we can rescale as follows:

$$\tau = \left[\frac{1}{24}(3\kappa - v)h'''\left(\frac{r}{2}\right)\right]t \tag{13}$$

$$R = -\frac{1 + (3\kappa - v)h'\left(\frac{r}{2}\right)}{\frac{1}{24}(3\kappa - v)h'''\left(\frac{r}{2}\right)} \tag{14}$$

which transforms (12) into the normal form of a supercritical pitchfork bifurcation, $ds/d\tau = Rs - s^3$, where the bifurcation occurs for $R = 0$, beyond which the symmetric $s = 0$ equilibrium is absolutely unstable and two stable asymmetric branches emerge [12].

When $h'''(r/2) < 0$, the pitchfork bifurcation is subcritical, exhibiting a hard loss of stability, multistability, and hysteresis. The relevant zero crossing of $h'''(x) = (-x^4 + 6x^2 - 3)e^{-\frac{1}{2}x^2}$ in marking the boundary between supercritical and subcritical bifurcations occurs at $x = (3 + \sqrt{6})^{1/2}$ corresponding to a discord of $r = 4.66$.

4.1 SHD Upper Boundary: κ_1

We now calculate the boundary in $\Delta\mu - \kappa$ parameter space given by the critical value of the coupling strength κ_1 at which the SHD state becomes absolutely unstable. Setting the coefficient of the first term on the righthand side of (12) equal to zero yields

$$\kappa = -\frac{1}{3h'(\frac{r}{2})} + \frac{v}{3}. \tag{15}$$

Substituting $r \approx \Delta\mu + \theta$, and expanding (15) to first order in θ gives

$$\kappa_1 \approx \frac{1}{3}\left\{\frac{1}{h'(\frac{\Delta\mu}{2})} - \frac{h''(\frac{\Delta\mu}{2})}{h'^2(\frac{\Delta\mu}{2})}\frac{\theta}{2}\right\} + \frac{v}{3} \tag{16}$$

The expression (11) for θ can be inserted into the above which, after rearranging, yields the characteristic equation

$$0 = 3h'(\frac{\Delta\mu}{2})\kappa_1^2 + \left(4 + M + 2vh'(\frac{\Delta\mu}{2})\right)\kappa_1 + \frac{1}{h'(\frac{\Delta\mu}{2})} + Mv - v^2h'(\frac{\Delta\mu}{2}), \tag{17}$$

where $M = \frac{\Delta\mu^4 - 12\Delta\mu^2}{(\Delta\mu^2-4)^2}$. This can be solved to give the following approximation for κ_1:

$$\kappa_1 \approx \frac{2}{3}\frac{e^{\frac{\Delta\mu^2}{8}}}{(\Delta\mu^2-4)}\left\{4 + M + 2vh'\left(\frac{\Delta\mu}{2}\right) - \left[4 + 8M + M^2 + 8vh'\left(\frac{\Delta\mu}{2}\right)\left(2 - M + 2vh'(\frac{\Delta\mu}{2})\right)\right]^{\frac{1}{2}}\right\}. \quad (18)$$

This increases rapidly as $\Delta\mu$ becomes very large. The appearance of v as a product with the very small $h'(\Delta\mu)$ implies that κ_1 will be nearly identical to the $v = 0$ case as $\Delta\mu$ gets large.

4.2 MR Lower Boundary in Subcritical Zone: κ_2

Turning now to the disappearance of the asymmetric solutions in the subcritical bifurcation regime, this corresponds to the transition between the multistable zone where the MR and SHD states coexist to the zone in which only the SHD state exists as the coupling strength is lowered. This transition occurs via a saddle-node bifurcation in which stable and unstable asymmetric equilibria collide. The associated bifurcation boundary κ_2 can be calculated by analyzing Eq. (7) around the MR equilibrium in which the minority node x_1 stays near its natural bias while the majority pair (x_2, x_3) is very nearly symmetrically positioned around the midpoint between their natural biases, $\Delta\mu/4$. Asymmetric coupling, $v \neq 0$, will shift the equilibrium mean of the majority rule pair by an amount given by $\varepsilon = (x_2 + x_3)/2 - \Delta\mu/4$. For large $\Delta\mu$, $x_2 - x_1 = (r - s)/2$ is large and we can neglect the term $h((r - s)/2)$ in Eq. (7). Accordingly, we make the approximations for the outer opinion coordinates: $x_1 \approx -\Delta\mu/2$ and $x_3 \approx \Delta\mu/2 + 2\varepsilon - x_2$. The asymmetry is then $s = x_3 - 2x_2 + x_3 = -3x_2 + 2\varepsilon$. Rearranging yields $x_2 = -s/3 + 2\varepsilon/3$ and then $x_3 = s/3 + \Delta\mu/2 + 4\varepsilon/3$ so that the discord can now be written in terms of s as $r = x_3 - x_1 = s/3 + \Delta\mu + 4\varepsilon/3$. The argument of the coupling function term retained from Eq. (7) is $(r + s)/2 = 2/3(s + 3/4\Delta\mu + \varepsilon)$. Finally, we transform to the variable $\tilde{s} = s + 3\Delta\mu/4 + \varepsilon$ and Eq. (7) becomes

$$\frac{d\tilde{s}}{dt} = -(\tilde{s} - \frac{3}{4}\Delta\mu - \varepsilon) - (3\kappa - v)h\left(\frac{2}{3}\tilde{s}\right). \quad (19)$$

Equation (8) can be used to calculate the shift ε in the mean of x_2 and x_3 (neglecting the $h((r - s)/2)$ term and using $x_1 = -\Delta\mu/2$) yielding $\varepsilon = -vh(\frac{r+s}{2}) = -vh(\frac{2}{3}\tilde{s})$. Taking $v \ll \kappa$, the first order contribution of v resulting from the last term in Eq. (19) is given by $vh(\frac{2}{3}\tilde{s})$ which cancels out the ε term. Thus, we get

$$\frac{d\tilde{s}}{dt} = -(\tilde{s} - \frac{3}{4}\Delta\mu) - 3\kappa h(\frac{2}{3}\tilde{s}), \tag{20}$$

and we see that the effect of asymmetric coupling between the center and the extremes disappears for small v and so will not impact the bifurcation boundary.

The equilibrium value for which the saddle-node bifurcation occurs is marked by the vanishing of the right-hand side of the above equation as well as its derivative, yielding upon rearrangement the conditions:

$$\tilde{s} - \frac{3}{4}\Delta\mu = -2\kappa_2\tilde{s}e^{-\frac{2}{9}\tilde{s}^2} \tag{21}$$

$$1 = -2\kappa_2(1 - \frac{4}{9}\tilde{s})e^{-\frac{2}{9}\tilde{s}^2}, \tag{22}$$

where κ_2 denotes the coupling strength at which the bifurcation occurs. Taking the ratio of (21) to (22) and rearranging yields the cubic equation

$$0 = \tilde{s}^3 - \frac{3}{4}\Delta\mu\tilde{s}^2 + \frac{27}{16}\Delta\mu. \tag{23}$$

For large $\Delta\mu$, it can be readily verified that to $O(\frac{1}{\Delta\mu})$, the solution to this equation is given by $\tilde{s} = 2(1 + \frac{1}{\Delta\mu})$. Employing (21) to solve for κ_2 and then substituting in this approximation for $\tilde{s}$ yields

$$\begin{aligned}\kappa_2 &= \frac{\frac{3}{4}\Delta\mu - \tilde{s}}{2\tilde{s}}^{\frac{2}{9}\tilde{s}^2} \\ &\approx \frac{1}{4}\frac{\Delta\mu^2 - 2\Delta\mu - 2}{\Delta\mu + 1}e^{\frac{1}{2}(1+\frac{1}{\Delta\mu})^2},\end{aligned} \tag{24}$$

which increases linearly to leading order in $\Delta\mu$. While the rapidly increasing κ_1 marks when the MR state will ensue from natural bias initial conditions, the linear dependence of κ_2 shows that the coupling strength for which a stable MR state is available does keep pace with $\Delta\mu$. This is significant because if a stochastic forcing is added to Eq. (3) to simulate random incoming external information for instance then transitions between states can occur in which the SHD state jumps to the MR state (and vice versa) as we have observed in simulations.

4.3 SLD Lower Boundary: κ_3

We now calculate the boundary κ_3 below which the SLD state given by $(r, s = 0)$ becomes absolutely unstable. The boundary can be calculated by using Eq. (9) and the coefficient of s in Eq. (12) to solve for r for which the system undergoes a pitchfork

bifurcation from the SLD equilibrium to the MR state. We obtain the conditions:

$$r - \Delta\mu = -(\kappa_3 + v) r e^{-r^2/8} \tag{25}$$

$$1 = -(3\kappa_3 - v)\left(1 - \frac{r^2}{4}\right) e^{-r^2/8}. \tag{26}$$

Neglecting small v, then taking the ratio of the above pair and rearranging gives

$$0 = r^3 - \Delta\mu r^2 - \frac{8}{3} r + 4\Delta\mu. \tag{27}$$

Near the bifurcation, the equilibrium discord for the SLD state is $r \approx 2$ and the solution to (27) to $O(1/\Delta\mu)$ is $r \approx 2 + 2/(3\Delta\mu)$. Using this in (25) enables us to calculate κ_3

$$\kappa_3 + v = -\frac{r - \Delta\mu}{r} e^{r^2/8} \tag{28}$$

$$\kappa_3 \approx \frac{\Delta\mu^2 - 2\Delta\mu + \frac{2}{3}}{2\Delta\mu + \frac{2}{3}} e^{\frac{1}{8}\left(2 + \frac{2}{3}\frac{1}{\Delta\mu}\right)^2} - v. \tag{29}$$

κ_3 shows a linear dependence for large $\Delta\mu$ as did κ_2 but, significantly, it also has a linear dependence upon small v.

4.4 Chain and Complete Stability Diagrams

Figure 3a displays the stability diagram of the chain network showing the regimes in $\Delta\mu - \kappa$ parameter space where the different outcomes are stable and the bound-

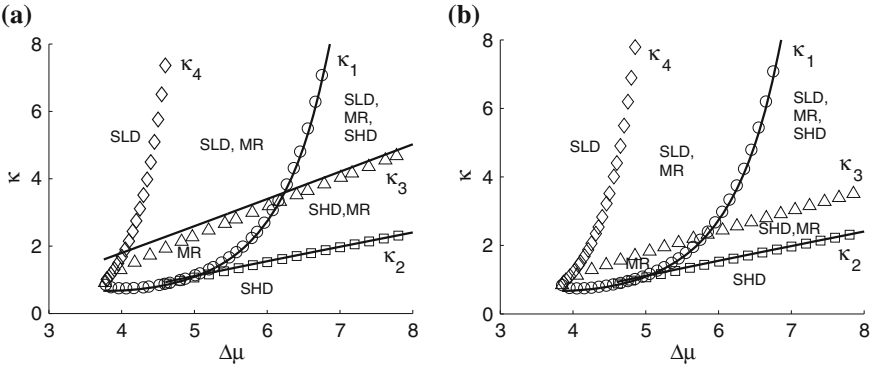

Fig. 3 Stability diagram of triad with symmetric coupling for: **a** chain network and **b** complete network. *Open markers* are numerically obtained boundaries. *Solid lines* are chain analytical approximations (18), (24), and (29) for κ_1, κ_2, and κ_3 respectively

aries between them. The open markers represent numerically-obtained bifurcation boundaries as found using the MATCONT software package for prediction-correction continuation [3]. The numerical curves agree very well with the analytical approximations (18), (24), and (29) for κ_1, κ_2, and κ_3 respectively, except in the immediate vicinity of the critical divergence. Also shown is the boundary κ_4 beyond which the MR state is no longer present. Note the presence of a substantial zone where only the MR state is stable. There are also multistable zones in which two or all three states are stable.

The stability diagram for the complete network is shown in Fig. 3b. For κ_1 and κ_2 the approximations derived for the chain network, (18) and (24), agree very well with the numerically-determined boundaries. This indicates that the coupling between the two outer nodes can be safely neglected due to their extremely disparate opinions in the SHD and MR states. However, the chain approximation for κ_3 is substantially higher than the complete network's κ_3. This is due to the significantly lower discord of the SLD state in the complete network, thereby making that state more robust. This reduces the size of the MR-only zone as compared with the chain. In addition, κ_4 shifts to the right in the complete network which has the effect of expanding the SLD-only zone.

For the asymmetric coupling case of $v < 0$, i.e., when the end nodes are more influential than the center node, κ_3 shifts upward as evident from (29) whereas κ_1 and κ_2 are nearly unchanged for large $\Delta\mu$. This decreases the size of the zone where the SLD state is stable and increases the size of the MR-only and MR-SHD zones as observed in simulations; in addition, the critical divergence shifts to lower values of $\Delta\mu$. For $v > 0$, κ_3 shifts downward and the critical divergence shifts to the right so that the MR-only and MR-SHD zones decrease in size. However, it is significant that skewed majority rule outcomes can arise even when the center node has greater influence than the end nodes.

5 Five-Node Networks

We have also observed majority rule outcomes in five node topologies as shown in Fig. 4. In the simulations, the natural biases are distributed uniformly over the range $\Delta\mu = 6$ and ordered so that $(\mu_1, \ldots, \mu_5) = (-3, -1.5, 0, 1.5, 3)$. Three different

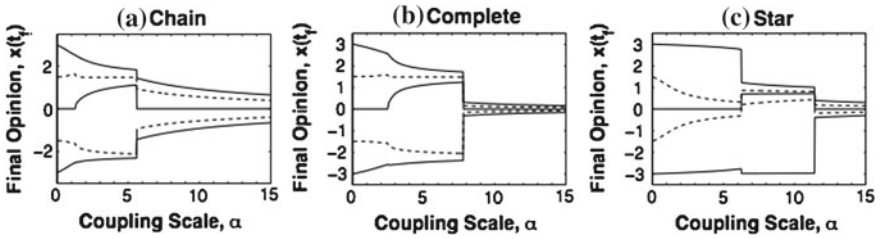

Fig. 4 Final node opinion versus coupling scale for five-node networks: **a** chain; **b** complete; **c** star. Simulation duration, $t_f = 200$

topologies are used: (1) the chain in which each node is connected only to its nearest neighbor along the opinion axis, $A_{ij} = \delta_{i,j\pm1}$; (2) the complete network where all nodes are connected to each other; and (3) the star in which the off-center nodes are only connected to the center node having $\mu_3 = 0$ so that $A_{i3} = A_{3i} = 1$ for $i \in 1, 2, 4, 5$ else $A_{ij} = 0$. The coupling strengths are identical for all ties, $\kappa_{ij} = \kappa A_{ij}$. But comparing the topologies for the same κ would allow topologies with more ties to have greater total coupling, thereby affording them a greater communication rate, for instance. Consequently, to compare topologies on a common basis, we relate the coupling strengths to the coupling scale α via the relationship $\kappa_{ij} = \alpha A_{ij}/\bar{d}$ where $\bar{d}$ is the mean degree, $\bar{d} = \sum_{i,j} A_{ij}/N$. From this form we see that α is equal to the average coupling strength, $\alpha = \sum_{i,j} \kappa_{ij}/N$. It is observed that in the MR state, the majority is 3-2 in the chain and complete networks whereas it is 4-1 in the star in which the intermediate negative node, x_2, is drawn upward into the positive x majority. We also note that the discontinuous transitions along the α axis occur first for the chain then the complete network and last for the star. The earlier transition to the SLD state for the chain network as compared with the star is striking since they both have the same number of directed edges, 12, and can be attributed to the fact that the couplings between the center and the outermost nodes present in the star are weaker compared with the only nearest-neighbor couplings in the chain; however, once achieved, the SLD state is much tighter in the star.

6 Conclusion

We have shown that an asymmetric outcome of majority rule arises from a symmetry-breaking pitchfork bifurcation using a model that is a nonlinear variant of the influential Friedkin-Johnsen model of opinion network dynamics. This symmetry-breaking route to majority rule only occurs for initial disagreements above the critical divergence. For lower disagreement, the more intuitive process of convergence toward the center applies as would be expected from the Friedkin-Johnsen model. This qualitative difference at low and high disagreement suggests that bifurcation-induced majority rule may be observable in laboratory experiments involving group discussion. Finally, we note that although there is a regime in which majority rule is predicted, the actual policy outcome in this regime is fundamentally unpredictable and may depend on relatively minor or random variables such as who speaks first.

Acknowledgments We acknowledge the support of the Defense Threat Reduction Agency and the Office of Naval Research under grant HDTRA1-10-1-0075.

References

1. C. Castellano, S. Fortunato, V. Loreto, Statistical physics of social dynamics. Rev. Mod. Phys. **81**, 591–646 (2009)
2. J.H. Davis, Group decision making and quantitative judgments: a consensus model, in *Understanding Group Behavior: Consensual Action by Small Groups*, ed. by E. Witte, J.H. Davis (Lawrence Erlbaum, Mahwah, 1996)
3. A. Dhooge, W. Govaerts, Y.A. Kuznetsov, Matcont: a MATLAB package for numerical bifurcation analysis of ODEs. ACM Trans. Math. Softw. **29**(2), 141–164 (2003)
4. A. Eagly, S. Chaiken, *The Psychology of Attitudes* (Harcourt, Fort Worth, 1993)
5. N.E. Friedkin, E.C. Johnsen, *Social Influence Network Theory: A Sociological Examination of Small Group Dynamics* (Cambridge University Press, Cambridge, 2011)
6. M. Gabbay, A dynamical systems model of small group decision making, in *Diplomacy Games*, ed. by R. Avenhaus, I.W. Zartman (Springer, Berlin, 2007)
7. M. Gabbay, The effects of nonlinear interactions and network structure in small group opinion dynamics. Phys. A Stat. Mech. Appl. **378**(1), 118–126 (2007)
8. J. Gastil, *The Group in Society* (Sage, Los Angeles, 2010)
9. M. Hinich, M. Munger, *Analytical Politics* (Cambridge University Press, Cambridge, 1997)
10. M. Mesbahi, M. Egerstedt, *Graph Theoretic Methods in Multiagent Networks* (Princeton University Press, Princeton, 2010)
11. V. Srivastava, J. Moehlis, F. Bullo, On bifurcations in nonlinear consensus networks. J. Nonlinear Sci. **21**, 875–895 (2011)
12. S.H. Strogatz, *Nonlinear Dynamics and Chaos* (Perseus Books, Reading, 1994)